ELSEVIER

Journal of Alloys and Compounds 317–318 (2001) 470–474

Journal of ALLOYS AND COMPOUNDS

www.elsevier.com/locate/jallcom

# Magnetic characteristics of $Er(Mn_{12-x}Fe_x)$ compounds ($x=7$, 9) determined by X-ray magnetic circular dichroism

M. Morales[a,*], M. Bacmann[a], Ch. Baudelet[b], A. Delobbe[b], D. Fruchart[a], Ch. Giorgetti[b], G. Krill[b], P. Wolfers[a]

[a]*Laboratoire de Cristallographie du CNRS, BP 166, 38042 Grenoble Cedex 9, France*

[b]*Laboratoire pour l'Utilisation du Rayonnement Synchrotron, Bat 209D, Université Paris-Sud, 91405 Orsay, France*

**Abstract**

The $RMn_{12-x}Fe_x$ series of compounds of $ThMn_{12}$ structure type exhibit particularly complicated and composition sensitive magnetic properties. Previous neutron diffraction and magnetisation experiments have permitted to relate the main features to the strength of the local magnetic moments (3d polarisation) and the nature exchange forces between the Mn, Fe and R sublattices. X-ray magnetic circular dichroism analyses have been undertaken on iron rich compounds with R=Er. They allow to better understand the thermal and field behaviour of the local magnetic moments as well as the nature of the magnetic couplings between the 3d metals. © 2001 Elsevier Science B.V. All rights reserved.

*Keywords:* Crystal and magnetic structure; 4f–3d Metal compounds; X-ray magnetic circular dichroism

## 1. Introduction

The series of compounds of formula $RFe_{12-y}M_y$ (where $y=12-x$, M=3d metal or Al, Si) of $ThMn_{12}$ structure type (SG: *I4/mmm*) [1] are mostly ferromagnetic (or ferrimagnetic) materials. The rare earth atom occupies the 2a position and the 3d atoms are distributed on three different sites 8f, 8i, 8j; in most cases the M atom substitutes preferentially in the 8i sites. The Curie temperature of this series is markedly dependent on the substitution rate *y*, and on the nature of both the transition and rare earth metals. If for selected parent carbides or nitrides hard magnet properties can be expected, namely with M=V and *y* varied between 1 and 2, with M=Mn, the magnetic properties are strongly affected by the manganese content. Neutron diffraction experiments have allowed to determine the scheme of substitution of Fe for Mn, more particularly on the R=Y, Nd, Ho, Er compounds. It is revealed to be random on two of the three d-element sites 8f, 8i, 8j of the structure, as seen in Fig. 1 [2]. Furthermore, the values of the mean magnetic moments ⟨Mn–Fe⟩, have been determined on the three sites.

A schematic magnetic phase diagram was derived which underlines three main magnetic behaviours as drawn in Fig. 2. Firstly, the $ErMn_{12}$ type of magnetic structures which extends from $x=0$ to $x\approx3$, results on the combination of basal non collinear antiferromagnetic arrangements setting on the Mn(Fe) sublattices with ferromagnetic Er moments oriented along the *c*-axis. Secondly, for $3\leq x\leq6$, the low temperature magnetic behaviour is more complex,

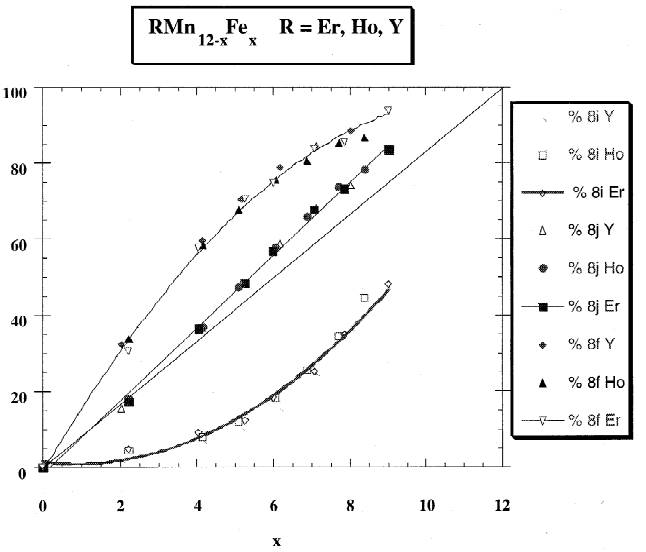


Fig. 1. Distribution of manganese and iron (*x*) in the three d sites 8f, 8i and 8j in $RMn_{12-x}Fe_x$ compounds for R=Y, Ho, Er as determined from neutron diffraction studies.

*Corresponding author. Fax: +33-4-7688-1038.

*E-mail address:* morales@labs.polycnrs-gre.fr (M. Morales).

0925-8388/01/$ – see front matter 
PII: S0925-8388(00)01372-4

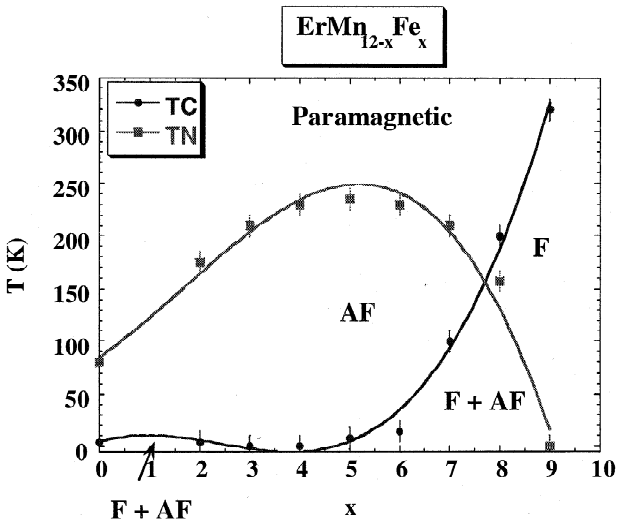


Fig. 2. Magnetic phase diagram of $ErMn_{12-x}Fe_x$ versus the substitution rate $x$ of Fe to Mn.

with a complete disappearance of long range ordering both on the Er sublattices and for some of the 3d magnetic components. Thirdly, for the Fe rich side of compounds ($x \geq 7$), stronger ferromagnetic couplings overpass the other types of magnetic exchange forces; hence ferrimagnetic behaviours are observed. The changes between complex to collinear magnetic arrangements have been first investigated by using magnetic neutron diffraction. Table 1 gathers the main characteristics of the magnetic structure for $x=7$ and 9. The magnetic arrangement determined by the basal components is non collinear of antiferromagnetic type and parent to the model described in Fig. 7 in Ref. [3].

## 2. Experimental

X-ray magnetic circular dichroism (XMCD) techniques were used to analyse the ferromagnetic components of the different elements Er, Mn and Fe. Particularly those of the atomic orbitals exhibiting a direct or indirect magnetic polarisation were checked for, since such a technique is chemical and orbital selective. For the relevant compound ($x=7$), the erbium XMCD signals have been recorded at the $L_{2,3}$ and $M_{4,5}$ absorption edges, respectively, checking the 5d and 4f levels, using the D11 and SU22 instruments setting at LURE, Orsay [4]. In the first case, the analysis was made in a transmission mode using a finely crushed sample deposited as a thin film, this is the opposite to the second case where the polished surface of a bulk sample was explored by absorption. Moreover, dichroic signals were also recorded on the two samples ($x=7$, 9), to analyse the $L_{2,3}$ absorption edges of Mn and Fe thus the 3d levels, by using the facilities of the SU23 reflection type instruments. In both cases of powder and bulk materials, the analysis was performed on randomly oriented magnetic domains. The dichroic signals were extracted from the difference of the two absorption curves, when applying successively a reverse magnetising field (along the photon beam) on the samples. More details on the used experimental set up can be found in the LURE technical handbook [4]. Reduction of the data was made accounting for several experimental parameters and physical criteria, e.g. the polarisation rate of the incident photons, the sum rules [5,6] that allow (within specific approximations) to extract the spin and orbital components to the moment of the considered shell (d or f). Furthermore, estimates of the number of holes in the valence band of the elements was made according to literature as well as when neglecting the role of the magnetic dipolar moment tensor (cubic Wigner–Seitz cell approximation).

Table 1
Parallel and perpendicular components of the magnetic structure of $ErMn_{12-x}Fe_x$ as determined at 4 K, and ordering temperatures

| Values in $\mu_B$/fu and directions of the magnetic moments on the different sites | $x=7$ | $x=9$ |
|---|---|---|
| $\mu_{8i}$ | 0.90 (2) | 0.38 (7) |
| $\theta_{8i}$ | 90° | 0° |
| $\mu_{8j}$ | 1.28 (7) | 1.61 (8) |
| $\theta_{8j}$ | 68.9° | 0° |
| $\mu_{8f}$ | 0.98 (5) | 1.50 (6) |
| $\theta_{8f}$ | 61.9° | 0° |
| $\mu_{2a}$ | −6.4 (1) | −7.7 (1) |
| $\theta_{2a}$ | 0° | 0° |
| Ordering temperatures (K) | | |
| $T_N$ | 210 | – |
| $T_C$ | 100 | 320 |

## 3. Results and discussion

At the Er $L_{2,3}$ absorption edge, experiments were successively undertaken at 5 and 100 K, apart from the temperature where magnetisation measurements reveal the rise of ferromagnetic components in $ErMn_5Fe_7$. For example, the $L_3$ signal is made of two lobes, negative and positive successively. At present it remains difficult to interpret unambiguously such data since the sum rules [5,6] are not exactly valid at this L edges, and because simultaneous quadrupolar (negative contribution) and dipolar (positive contribution) transitions involve this orbital. However, owing to the 5d character of the presently analysed level, the signal evidenced at 5 K remaining clearly visible at 100 K, even if weak, leads to assert that a ferromagnetic polarisation stand above the so-called Curie temperature $T_C$ ($\leq$100 K) as seen in Fig. 2.

From the positive sign of the $M_5$ XMCD signal (analysis of the $M_{4,5}$ edge of $ErMn_5Fe_7$ on SU22), it can be deduced that the kinetic moment $J$ is antiparallel to the applied magnetic field. This is consistent with Table 1, and in rather good agreement with the magnetisation measure-

ments [7] that indicate a weak saturation moment ($T \rightarrow 0$, $H \rightarrow 0$, $M \approx 1\ \mu_B$). The thermal and field behaviours of this signal were measured between $T = 12$ and 100 K for $H = 1$ T and from $H = 0$ to 6 T at 12 K, respectively. The magnetic signals were normalised to the 4f magnetic moment reference to a multiplet theory derived estimation, and to a saturation value of 9 $\mu_B$. Fig. 3a and b, respectively, show these variations that agree well with the thermal behaviour ($T_C \approx 90$–100 K) on one side and the bulk magnetisation behaviour $M(H)$ on the other side. In fact, owing to the relatively strong magneto-crystalline anisotropy setting on this type of compounds, a random distribution of the easy directions (powder type distribution in the sample), a complete coherent rotation of magnetisation within the domain needs to apply much larger magnetic fields, as systematically observed from bulk magnetisation experiments.

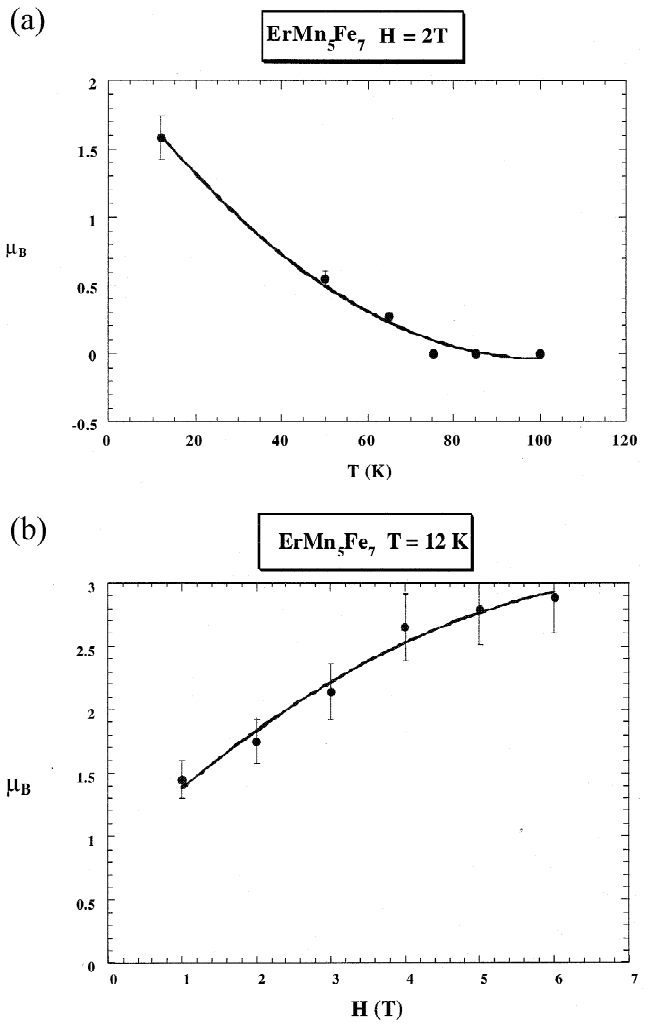


Fig. 3. (a) Thermal behaviour of the 4f erbium magnetic component along the applied magnetic field of 2 T, as fitted from the data of the $M_5$-XMCD edge of $ErMn_5Fe_7$. (b) Behaviour of the 4f erbium magnetic component at 12 K, along the applied magnetic field up to 6 T, as fitted from the $M_5$ XMCD edge of $ErMn_5Fe_7$.

The $L_{2,3}$ Fe and Mn edges were checked versus temperature and applied field both for the $ErMn_5Fe_7$ and $ErMn_3Fe_9$ samples. For the first one compound, the dichroic signal was found almost null at the Mn edge, and weak at the Fe one. An estimate of the corresponding ferromagnetically polarised mean moment onto the Fe sublattices leads to a small value (a few tenths of $\mu_B$ at $T = 5$ K and under $H = 6$ T) in reasonable agreement with the values of 0.45 $\mu_B$ found along the *c*-axis, as measured by neutron diffraction onto the 8f and 8j sites only (the 8i site does not share any ferromagnetic component, see Table 1).

For $ErMn_3Fe_9$, XMCD signals were clearly evidenced both at the Mn and Fe edges. The $L_{2,3}$ signals measured at 4 K under a field of 5.5 T are represented in Fig. 4a and b. The signal measured at the Mn edge is about three times smaller than that found at the Fe one, but surprisingly the magnetic polarisation are of opposite signs. Moreover, it is deduced that the magnetisation (opposite to the 3d spin) of iron (manganese) is parallel (antiparallel) to the applied magnetic field. The Mn–Fe exchange couplings setting on the 3d sites are essentially of a ferrimagnetic type. In fact these couplings mostly concern the 8i site with the two other ones (8j and 8f) since the relative occupation numbers of manganese are, respectively, of 52, 16.5 and 6.5%. Application of the sum rules [5,6] allows the determination of the projected components along applied the magnetic field ($H = 5.5$ T) of the spin, orbital and total parts for manganese and iron. The corresponding values are reported in Table 2 for temperatures of 4, 35 and 80 K, respectively. If the contribution to magnetisation on Fe remains almost constant when temperature increases, that of Mn markedly drops. Nevertheless, this unexpected result is fully consistent with the thermal variation of the local ferromagnetic components determined from neutron diffraction as represented in Fig. 5. The anomaly in the mean ferromagnetic contribution measured on the 8i, 8j and 8f 3d sites (decreasing strength of anomalies from i to f sites) down to about 80 K can be fairly explained accounting for the local and opposite magnetic polarisation of Mn and Fe d moments. The variations measured at 4 K versus the applied magnetic field are plotted in Fig. 6a and b. Extrapolation at infinite field gives 1.4 $\mu_B$ for Fe and at zero field it is 0.4 $\mu_B$ for Mn. It is worth noting that the Er–Er ferromagnetic couplings are no longer efficient (80–100 K); some tens of degrees higher results in the loss of the ferromagnetic polarisation on Mn (mainly on the 8i sites).

## 4. Conclusion

Knowledge of the complicated characteristics of the $RMn_{12-x}Fe_x$ series of compounds was previously deduced from extended magnetisation and neutron diffraction experiments [7]. However, some of the pertinent parameters

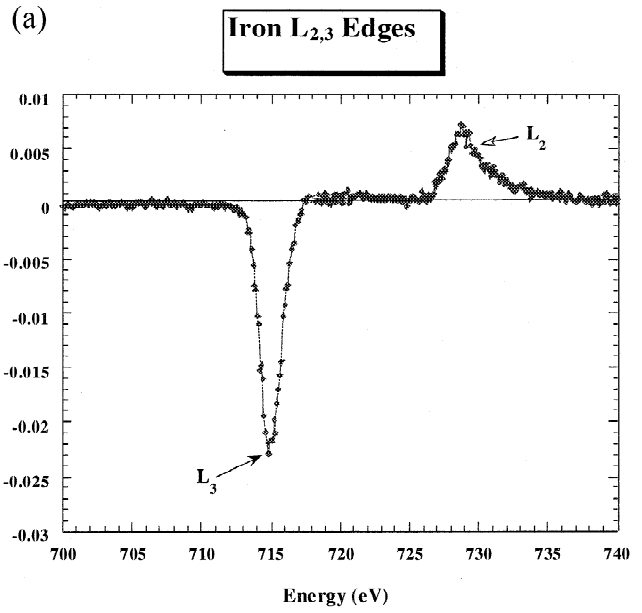


Fig. 4. (a) XMCD signal at the $L_{2,3}$ edge of iron in $ErMn_3Fe_9$, for $T=4$ K, under $H=5.5$ T. (b) XMCD signal at the $L_{2,3}$ edge of manganese in $ErMn_3Fe_9$, for $T=4$ K, under $H=5.5$ T.

Table 2
Components of the projected moments along the applied magnetic field direction

| T (K) | Magnetic moments ($\mu_B$/atom) | | | | | |
|---|---|---|---|---|---|---|
| | Iron | | | Manganese | | |
| | $\mu$ ($L_z$) | $\mu$ ($S_z$) | $\mu$ (total) | $\mu$ ($L_z$) | $\mu$ ($S_z$) | $\mu$ (total) |
| 4 | 0.02 | 1.19 | 1.21 | −0.02 | −0.39 | −0.41 |
| 35 | 0.12 | 1.00 | 1.12 | −0.14 | −0.22 | −0.36 |
| 80 | 0.12 | 1.00 | 1.12 | −0.09 | −0.10 | −0.19 |

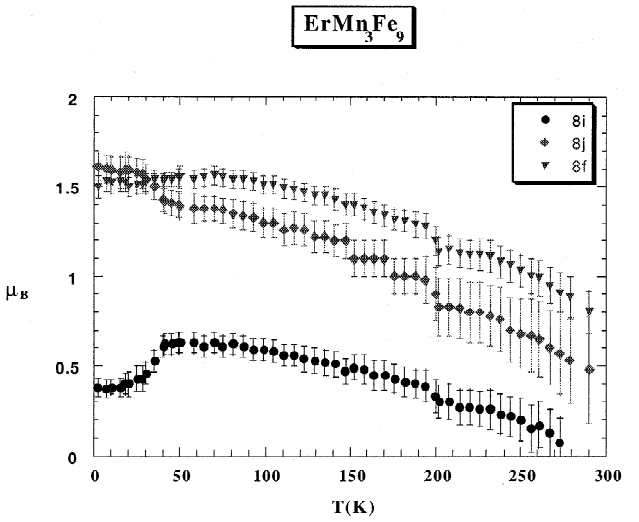


Fig. 5. Behaviour of the magnetic 3d (Mn,Fe) moments refined from neutron diffraction data on the 8f, 8i and 8j sites in $ErMn_3Fe_9$.

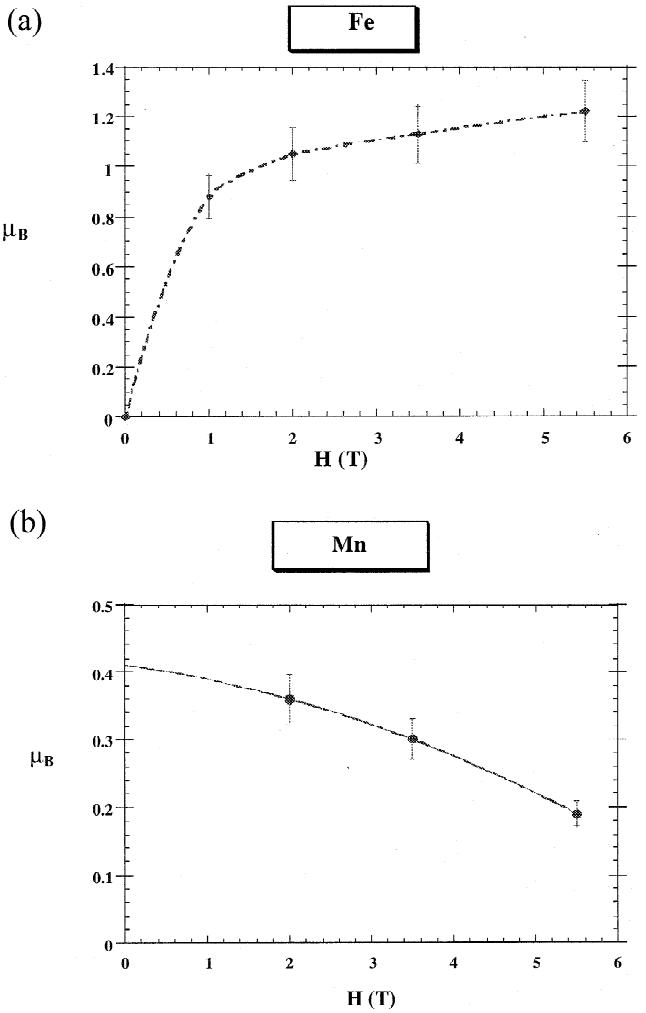


Fig. 6. (a) Field behaviour at $T=4$ K of the magnetic component of iron as fitted from the data of the XMCD-$L_{2,3}$ edge of $ErMn_3Fe_9$. (b) Field behaviour at $T=4$ K of the magnetic component of manganese as fitted from the data of the XMCD-$L_{2,3}$ edge of $ErMn_3Fe_9$.

were determined as bulk or mean value quantities. Using the XMCD techniques for the first time on some members of the series (R = Er, $x = 7$ and 9), relevant information has been deduced, enlightening the thermal- and field-dependent behaviour of the ferromagnetic polarisation on Er, Mn and Fe, both with the main aspect of the Mn–Fe exchange coupling.

## References

[1] J.V. Florio, N.C. Baenziger, R.E. Rundle, Acta Crystallogr. 9 (1956) 367–372.
[2] M. Artigas, M. Bacmann, D. Fruchart, M. Morales, E. Tomey, Physica B 234–236 (1997) 155–156.
[3] M. Morales, M. Artigas, M. Bacmann, D. Fruchart, J.L. Soubeyroux, P. Wolfers, J. Alloys Comp. 262–263 (1997) 134–140.
[4] LURE, Technical User's Handbook (Guide Technique), LURE, Orsay, France, 1992.
[5] B.T. Thole, P. Carra, F. Sette, G. van der Laan, Phys. Rev. Lett. 68 (1992) 1943.
[6] P. Carra, B.T. Thole, M. Altarelli, X. Wang, Phys. Rev. B 70 (1993) 694.
[7] M. Morales, Thesis, Université J. Fourier, Grenoble, France, 1999.